Published in final edited form as:
J Inherit Metab Dis. 2010 December ; 33(0 3): S481–S487. doi:10.1007/s10545-010-9246-8.

Novel ETF dehydrogenase mutations in a patient with mild glutaric aciduria type II and complex II-III deficiency in liver and muscle

Lynne A. Wolfe,
Division of Medical Genetics, Department of Pediatrics, Children's Hospital of UPMC, Pittsburgh, PA, USA; Undiagnosed Diseases Program, National Human Genome Research Institute, Bethesda, MD, USA

Miao He,
Department of Human Genetics, Emory University, School of Medicine, Decatur, GA, USA

Jerry Vockley,
Division of Medical Genetics, Department of Pediatrics, Children's Hospital of UPMC, Pittsburgh, PA, USA; Department of Pediatrics, University of Pittsburgh, School of Medicine, Pittsburgh, PA, USA; Department of Human Genetics, University of Pittsburgh Graduate School of Public Health, Pittsburgh, PA, USA

Nicole Payne,
Division of Medical Genetics, Department of Pediatrics, Children's Hospital of UPMC, Pittsburgh, PA, USA

William Rhead,
Department of Pediatrics, Division of Clinical Genetics, Medical College of Wisconsin, Milwaukee, WI, USA

Charles Hoppel,
Department of Medicine, Louis Stokes Cleveland Department of Veterans Affairs Medical Center, Case Western Reserve University, Cleveland, OH, USA

Elaine Spector,
UCD DNA Diagnostic Laboratory, Aurora, CO, USA

Kim Gernert, and
BimCore/Biomolecular Computing Resource, Emory University School of Medicine, Atlanta, GA, USA

K. Michael Gibson
Division of Medical Genetics, Department of Pediatrics, Children's Hospital of UPMC, Pittsburgh, PA, USA; Department of Pediatrics, University of Pittsburgh, School of Medicine, Pittsburgh, PA, USA; Department of Human Genetics, University of Pittsburgh Graduate School of Public Health, Pittsburgh, PA, USA; Department of Pathology, Children's Hospital of UPMC, Pittsburgh, PA, USA; Department of Biological Sciences, Michigan Technological University, Room 740 DOW ESE Building, 1400 Townsend Drive, Houghton, MI, USA

kmgibson@mtu.edu.

Communicated by: Michael J. Bennett

Competing interest: None declared.

Abstract

We describe a 22-year-old male who developed severe hypoglycemia and lethargy during an acute illness at 4 months of age and subsequently grew and developed normally. At age 4 years he developed recurrent vomiting with mild hyperammonemia and dehydration requiring frequent hospitalizations. Glutaric aciduria Type II was suspected based upon biochemical findings and managed with cornstarch, carnitine and riboflavin supplements. He did not experience metabolic crises between ages 4-12 years. He experienced recurrent vomiting, mild hyperammonemia, and generalized weakness associated with acute illnesses and growth spurts. At age 18 years, he developed exercise intolerance and proximal muscle weakness leading to the identification of multiple acyl-CoAdehydrogenase and complex II/III deficiencies in both skeletal muscle and liver. Subsequent molecular characterization of the ETFDH gene revealed novel heterozygous mutations, p.G274X:c.820 G>T (exon 7) and p.P534L: c.1601 C>T (exon 12), the latter within the iron sulfur-cluster and predicted to affect ubiquinone reductase activity of ETFDH and the docking of ETF to ETFDH. Our case supports the concept of a structural interaction between ETFDH and other enzyme partners, and suggests that the conformational change upon ETF binding to ETFDH may play a key role in linking ETFDH to II/III super-complex formation.

Introduction

Glutaric Aciduria Type II (GAII; multiple acyl CoA dehydrogenase deficiency; OMIM 231680; 231675) is an autosomal-recessively inherited disorder of amino and fatty acid metabolism resulting from defects in at least two flavoproteins; electron-transfer flavoprotein (ETF; ETFDH) or electron-transfer flavoprotein ubiquinone oxidoreductase (ETF:QO) (Liang et al. 2009; Henriques et al. 2009; Law et al. 2009; Schiff et al. 2006; Frerman 1987). Within the mitochondria, soluble ETF accepts electrons from multiple oxidoreductases involved in fat metabolism. These electrons are subsequently shuttled to ETF-Q0, which is situated on the inner mitochondrial membrane, and eventually are transferred to ubiquinone within the oxidative phosphorylation system (e.g., respiratory chain). The central position of both ETFDH and ETF-Q0 in the oxidation-reduction reactions of the cellular milieu (ETF receives reducing equivalents from at least 10 oxidoreductases) has led to the concept of supercomplex formation between ETF and a number of structurally unique partners, including complexes of the oxidative phosphorylation system (Toogood et al. 2007; Henriques et al. 2009).

GAII manifests substantial clinical heterogeneity, from mild and late-onset forms to severe modalities associated with myopathy, cardiomyopathy, pancreatitis, and congenital anomalies. Episodic decompensation, including encephalopathy, lethargy, vomiting, hypoglycemia and hyperammonemia (with or without organomegaly) can lead to death. Similarly, metabolic heterogeneity can represent significant challenges in the diagnostic laboratory, and biochemical manifestations (glycine conjugates, sarcosine, others) may be absent. Additionally, plasma acylcarnitine analysis may not provide the definitive diagnosis, depending upon the metabolic status of the patient. The recent development of molecular diagnostics focused on the ETFDH and ETF-Q0 genes has proven beneficial in terms of achieving the final diagnosis for diagnostically-challenging patients.

Patients with GAII may manifest alterations in activities of the oxidative phosphorylation system (Santer et al. 1995), consistent with the interaction of ETFDH and ETF-Q0 with these systems. The proximal muscle weakness and pain occasionally noted in GAII has been ascribed to perturbations of the oxidative phosphorylation system correlated with primary abnormalities in the ETF systems (Law et al. 2009; Beresford et al. 2006). In the current report, we describe an adult male whose molecularly confirmed GAII associated with significant complex II and III deficiencies localized to skeletal muscle and liver. One of two

mutations in our patient's ETFDH gene resides within the ubiquinone binding region, providing support for a potential association between ETFDH and complexes II/III at the level of the ubiquinone binding site.

Materials and methods

All procedures occurred during a planned clinical evaluation, off all supplements and while metabolically stable, accompanied by informed consent from either the patient or guardian. Routine analyses of lactate, pyruvate, ammonia, carnitine, plasma and urine amino acids, plasma acylcarnitines, urine organic acids, and urine acylglycines were analyzed using standard procedures (Rinaldo et al. 2005). Similarly, light and electron microscopy of liver and muscle tissue followed established protocols for pathological evaluation. In vitro evaluation of fatty acid oxidation using HPLC coupled with either radiolabeled or stable-isotope probes (carnitine, branched chain amino acids, palmitate) was performed as described (Schmidt-Sommerfeld et al. 1998). Fatty acid oxidation and measurement of oxidative phosphorylation (complexes I-IV and citrate synthase) were performed according to published protocols (King et al. 2007; Chen et al. 2007). Evaluation of ornithine transcarbamylase in liver homogenates followed published methodology (Klein et al. 2008). Molecular analyses of the ETF a and b subunits (15q23-25; 19q13.3) and ETFDH (4q32qter) genes were performed in cultured leukocytes isolated from whole blood as described.

Homology modeling of human wild type and mutant ETFDH

Molecular modeling of *human* ETFDH was completed using Modeler (version 9v7; University of California San Francisco; http://salilab.org/modeler/) for model construction and SYBYL (version 8.0; Tripos, http://www.tripos.com) for analysis and refinement. The ETFDH model was built and minimized based on a sequence alignment and structural information from *porcine* ETF-QO (PDB entry 2gmh) (Zhang et al. 2006). Initial sequence alignments were obtained from the SwissModel server (http://swissmodel.expasy.org/; Arnold et al. 2006)and confirmed usingBlast to PDB (http://blast.ncbi.nlm.nih.gov/Blast.cgi) and ClustalW (http://searchlauncher.bcm.tmc.edu/multi-align/multi-align.html). The alignment showed 95% sequence identity and 97% conservation. All protein structure images were generated in Sybyl by Tripos (http://www.tripos.com).

Case report

The proband was the offspring of a gravida 2, para 2, AB 1 mother. Pregnancy was uneventful and free from any prenatal exposures. Delivery at 38 weeks was uneventful. Per report he spent the first several hours of life under observation in the NICU for mild respiratory distress. Birth measurements: head circumference and length were unknown; birth weight 6 pounds, 12 ounces (50th centile). The proband was discharged to home with his mother at 72 hours of age with no post-natal jaundice or hypoglycemia. He achieved all developmental milestones and received all vaccinations without any difficulties until his first viral illness at 4 months of age. There was no known consanguinity and a three-generation pedigree revealed a non-contributory family history. Maternal ethnicity was reported as German, Irish and English and paternal ethnicity as Italian and Irish.

At age 4 years he developed recurrent vomiting associated with mild hyperammonemia and dehydration requiring frequent hospitalizations for IV fluids. At this time, fibroblasts studies suggested glutaric aciduria Type II, and accordingly he was managed with fat and protein-restriction and cornstarch supplements. He did not experience any metabolic crisis or hospitalizations between the ages of 4-12 years when he was noted to experience recurrent

vomiting, mild hyperammonemia without hypoglycemia, and generalized weakness especially with acute illnesses and growth spurts. At approximately age 18 years, he developed recurrent vomiting, exercise intolerance and proximal muscle weakness leading to further extensive metabolic evaluation, which suggested anomalies of oxidative phosphorylation and acyl-CoA dehydrogenation in both skeletal muscle and liver (see below).

There was subsequent improvement in symptoms with dietary adjustment including the discontinuation of protein and fat restriction, as well as insertion of a GT for continuous feeds during illnesses. Riboflavin (100 mg daily), coenzyme Q (ubiquinol, 3 × 100 mg daily, Tishcon Corp.), carnitine (50 mg/kg/day) and Zofran (as needed) were prescribed and served to ameliorate recurrent vomiting, dehydration and muscle weakness.

Results

Metabolic studies

Blood and urine amino acids, carnitine, glucose, lactate and pyruvate, creatine kinase and plasma ubiquinone levels were within normal limits when well and only creatine kinase was elevated during illnesses. Plasma acylcarnitines were variable, being both normal and in one instance suggestive of very-long chain acyl-CoA dehydrogenase deficiency. Urine acylglycines revealed increased excretion of ethylmalonate and hexanoylglycine, while excretion of the latter was variable during repetitive urine organic acid studies. Blood ammonia levels were slightly increased when well (45-99 mmol/L, nl<38) and during acute illness (73-144 mmol/L).

Pathology

Light microscopy evaluation of skeletal muscle and skin were unremarkable. Electron microscopy of biopsied liver revealed mild, chronic inflammatory infiltrates with normal architecture and portal tracts; otherwise, no other pathological processes were noted. Approximately 30% of the liver specimen demonstrated mixed macro-micro-steatosis. Electron microscopy of skeletal muscle demonstrated rare small fibers without hypertrophy, inflammation or fibrosis. There were no internalized nuclei, central cores, split, moth-eaten or red-ragged fibers. NADH, SDH (succinate dehydrogenase) and PAS (periodic acid Schiff) stains were normal. Oil Red O staining demonstrated occasionally increased lipids felt to be within normal limits. COX (cytochrome oxidase) staining revealed rare pale fibers.

Enzymatic

Initial in vitro probe analyses (employing ^{3}H-carnitine, palmitate and branched chain amino acids) employing intact fibroblasts and HPLC separation of ^{3}H-carnitine esters suggested “mild” GA II, but this could not be confirmed using similar methodology in another laboratory, and ETFDH/ETF-QO enzyme activities and Western blot analyses in cultured fibroblasts were within normal limits. Evaluation of fibroblast oxidative phosphorylation activity (complexes I-IV) demonstrated normal activities throughout (data not shown). Characterization of complexes I-IV in skeletal muscle homogenates indicated deficiencies of complexes II-IV, but these findings were in the context of low citrate synthase activity (Table 1). Characterization of oxidative phosphorylation complexes in liver homogenates indicated deficiencies of complexes II and III with normal citrate synthase activity (Table 1).

Acyl-CoA dehydrogenases (ACDs) were also examined in homogenates of skeletal muscle and liver (Table 2). In both tissues, abnormalities of short-chain and long-chain ACDs were observed, in conjunction with decreased short-chain 3-ketothiolase activities. As for the case of skeletal muscle oxidative phosphorylation enzymes, citrate synthase (control enzyme)

was also low in this tissue for the ACD studies, but not in the liver. This was consistent with decreased mitochondrial number in skeletal muscle. Finally, chronic yet mild hyperammonemia prompted an evaluation of urea cycle enzymes in liver homogenates. Carbamyl phosphate synthase activity was within normal limits (data not shown), whereas ornithine transcarbamylase (OTC) activity was at the bottom of the parallel control range (patient 63.2 mmol/g liver/min; control 70.1±9.7 (SEM); parallel control with patient, 89.9). Muscle ubiquinone analysis was not completed due to insufficient available tissue. Additionally, we had hoped to evaluate complex II holoenzyme (using Western blot with blue native gel electrophoresis) and complex III, in order to correlate these results with the severe deficiencies observed enzymatically (Table 2), but again sufficient tissue samples were unavailable.

Molecular

Both cDNA and genomic DNA-based PCR amplifications and sequence analysis of the human ETFa, ETFb and ETFDH genes were performed essentially as described previously (Schiff et al. 2006). Identification of nucleotides and amino acids was based upon the cDNA sequence of ETFDH (NM_004453.1). The initiating ATG codon was numbered as bp 1–3, and the initiating methionine was subsequently numbered as amino acid 1. Two novel ETFDH mutations were identified; p.G274X and p.P534L and confirmed in parental DNA samples.

Mutation modeling

Human ETFDH models were constructed using the published porcine ETFDH crystal structure as template. All residues that differ between porcine and human were closely examined for structural disturbances. Overall, the backbone of the human model correlated well with that of the porcine ETFDH structure, and no major structural disturbances were observed in the human ETFDH model (Fig. 1a). Mutation p.P534L was introduced and the mutant p.P534L model was constructed in the same way as the wild type structure. Figure 1b depicts the overlay of porcine (red) and human mutant p. P534L ETFDH structures (white). In the wild type backbone structure, P534 is in direct contact with β-sheet 7 (residues 221-223); accordingly, the change of P534 to leucine with a longer side chain will either change the conformation of the loop that P534 resides in, as shown in the mutant model (Fig. 1b), or disrupt the conformation of the β-sheet 7, indicated by pink arrow, and this will significantly disrupt the interactions of His 529 and His 536 with C586. C586 is a pivotal residue for the function of the iron cluster. Of interest, rotation of the model to a different angle (Fig. 1c) reveals that the β-sheet 7 is actually a component of a large flat surface (indicated by the arrow). Figure 1d shows the frontal view of this flat surface area of ETFDH as highlighted by the white square. Since ETF directly transfers electrons to the iron-sulfur cluster, the observation that this flat surface on ETFDH is in close proximity to the iron-cluster region lends credence to our hypothesis that this is likely the docking site for ETF dimer.

Discussion

Glutaric aciduria type II may present a considerable diagnostic conundrum, and our patient is no exception. Absolute confirmation of the diagnosis did not occur until 22 years of age, although features of cyclical vomiting, proximal muscle weakness exacerbated by illness, exercise intolerance and fatigue were suggestive of GAII (Olsen et al. 2007; Gempel et al. 2007). Some patients have progressed to respiratory failure requiring mechanical ventilation that was reversible following riboflavin supplementation (Olsen et al. 2007). Adding to the diagnostic dilemmas were his very inconsistent metabolic features, that included mild yet persistent hyperammonemia, inconsistent acylcarnitine findings, and a variable excretion of

only hexanoylglycine in urine (Law et al. 2009; Olsen et al. 2007). Of note, dicarboxylic aciduria and elevated lactates were not observed, free carnitines and creatine kinase were within normal limits throughout, and he was never ketotic; likewise, sarcosine was never detected on routine blood amino acid analysis.

Microscopic analysis of biopsied liver suggested the presence of mild fat infiltration, consistent with the lipid-storage myopathies observed in other patients (Olsen et al. 2007). Modest defects in acyl-CoA dehydrogenases were observed in both liver and skeletal muscle, primarily in short- and long-chain ACDs, with more pronounced defects in the short-chain ketothiolase activities (Table 2). These results accompanied more severe abnormalities in complexes II-IV of the respiratory chain, not unlike that seen in other patients with GAII (Santer et al. 1995). However, the chronically low marker of tissue viability (citrate synthase) in skeletal muscle suggested that the overall mitochondrial number was decreased. Complicating the enzymatic studies was the observation of slightly decreased OTC activity in biopsied liver. The latter may have explained his mild but chronic hyperammonemia, but it is tempting to speculate that his inherited mitochondrial dysfunction (at the level of ETFDH) was causally linked to a mild defect in urea-genesis, as has been suggested by others (Bonham et al. 1999; Treem and Sokol 1998).

ETFDH is necessary for electron transport between ACDs and the flavin containing electron transport chain complexes (Olsen et al. 2007: Zhang et al. 2006). This has recently spurred the concept of supercomplex formation between ETFDH and complexes of oxidative phosphorylation (Henriques et al. 2009; Toogood et al. 2007). As elegantly outlined by Toogood and coworkers (Toogood et al. 2007), the FAD domain of ETF is “fluid” and assumes conformational changes that can recognize a variety of electron transfer flavoprotein partners. Ubiquinone is the physiological electron acceptor for ETFDH and transfer electrons to the cytochrome *bc*1 complex (complex III). ETFDH contains two redox active center, a [4Fe-4 S]$^{2+1+}$ cluster and a single equivalent of FAD. Interestingly, mutations that decrease midpoint potential of the iron cluster will decrease the ubiquinone reductase activity (Usselman et al. 2008), without altering the FAD midpoint potential. While the majority of GAII patients have novel mutations that cluster around the FAD binding site, our patient harbors a mutation directly within the iron cluster as shown in Fig. 1b, and it is therefore expected to alter the ubiquinone reductase activity. Since this residue is also close to the surface that we predict to be the ETF docking site, the p.P534L mutation may also disrupt the interaction between ETF and ETFDH, therefore the proper conformational change can not be achieved in order to pass the electron to ubiquinone or form a supercomplex with mitochondrial respiratory complexes, especially complex III. Curiously, mutations in this area of the iron-sulfur cluster binding domain were previously reported to disrupt the ubiquinone reductase activity of ETFDH, but those mutant proteins may still transfer electrons from ETF to the flavin ring of FAD in ETFDH (Beard et al. 1995). A limited number of riboflavin-responsive patients have demonstrated mutations in proximity to the iron-sulfur cluster of ETFDH (Olsen et al. 2007), and their clinical features of cyclical vomiting and learning difficulties are reminiscent of our patient’s phenotype. Although not functionally tested, it remains probable that the p.P534L mutation significantly disturbs ubiquinone reducing activity within ETFDH, and is directly responsible for the multilevel mitochondrial disruption observed in our patient. Identification of additional mutations in this region in subsequent GAII patients will provide further data to support our prediction.

Acknowledgments

The authors gratefully acknowledge the assistance of Drs. Frank Frerman, Stephen Goodman, Nancy Leslie, Dietrich Matern, Mendel Tuchman and Ms. Lorna Cropcho in the work-up and evaluation of this patient.

References

Arnold K, Bordoli L, Kopp J, Schwede T. The SWISS-MODEL workspace: a web-based environment for protein structure homology modeling. Bioinformatics. 2006; 22:195–201. [PubMed: 16301204]

Beard SE, Goodman SI, Bemelen K, Frerman FE. Characterization of a mutation that abolishes quinone reduction by electron transfer flavorprotein-ubiquinone oxidoreductase. Hum Mol Genet. 1995; 4:157–161. [PubMed: 7757062]

Beresford MW, Pourfarzam M, Turnbull DM, Davidson JE. So doctor, what exactly is wrong with my muscles? Glutaric aciduria type II presenting in a teenager. Neuromuscul Disord. 2006; 16:269–73. [PubMed: 16527485]

Bonham JR, Guthrie P, Downing M, Allen JC, Tanner MS, Sharrard M, Rittey C, Land JM, Fensom A, O'Neill D, Duley JA, Fairbanks LD. The allopurinol load test lacks specificity for primary urea cycle defects but may indicate unrecognized mitochondrial disease. J Inherit Metab Dis. 1999; 22:174–84. [PubMed: 10234613]

Chen Q, Camara AK, Stowe DF, Hoppel CL, Lesnefsky EJ. Modulation of electron transport protects cardiac mitochondria and decreases myocardial injury during ischemia and reperfusion. Am J Physiol Cell Physiol. 2007; 292:C137–47. [PubMed: 16971498]

Frerman FE. Reaction of electron-transfer flavoprotein ubiquinone oxidoreductase with mitochondrial respiratory chain. Biochimica et Biophysica Acta. 1987:161–169. [PubMed: 3620453]

Gempel K, Topaloglu H, Talim B, Schneiderat P, Schoser BGH, Hans VH, Palmafy B, Kale G, Tokatli A, Quinzii C, Hirano M, Naini A, DiMauro S, Prokisch H, Lochmuller H, Horvath R. The myopathic from of coenzyme CoQ deficiency is caused by mutations in the electron-transferring-flavoprotein dehydrogenase (ETFDH) gene. Brain. 2007; 130:2037–2044. [PubMed: 17412732]

Henriques BJ, Rodrigues JV, Olsen RK, Bross P, Gomes CM. Role of flavinylation in a mild variant of multiple acyl-CoA dehydrogenation deficiency: a molecular rationale for the effects of riboflavin supplementation. J Biol Chem. 2009; 284:4222–9. [PubMed: 19088074]

King KL, Stanley WC, Rosca M, Kerner J, Hoppel CL, Febbraio M. Fatty acid oxidation in cardiac and skeletal muscle mitochondria is unaffected by deletion of CD36. Arch Biochem Biophys. 2007; 467:234–8. [PubMed: 17904092]

Klein OD, Kostiner DR, Weisiger K, Moffatt E, Lindeman N, Goodman S, Tuchman M, Packman S. Acute fatal presentation of ornithine transcarbamylase deficiency in a previously healthy male. Hepatol Int. 2008:2390–4.

Law LK, Tang NL, Hui J, Fung SL, Ruiter J, Wanders RJ, Fok TF, Lam CW. Novel mutations in ETFDH gene in Chinese patients with riboflavin-responsive multiple acyl-CoA dehydrogenase deficiency. Clin Chim Acta. 2009; 404:95–99. [PubMed: 19265687]

Liang WC, Ohkuma A, Hayashi YK, López LC, Hirano M, Nonaka I, Noguchi S, Chen LH, Jong YJ, Nishino I. ETFDH mutations, CoQ10 levels, and respiratory chain activities in patients with riboflavin-responsive multiple acyl-CoA dehydrogenase deficiency. Neuromuscul Disord. 2009; 19:212–6. [PubMed: 19249206]

Olsen RK, Olpin SE, Andresen BS, Miedzybrodzka ZH, Pourfarzam M, Merinero B, Frerman FE, Beresford MW, Dean JCS, Cornelius N, Andersen O, Oldfors A, Holme E, Gregorsen N, Turnball DM, Morris AAM. ETFDH mutations as a major cause of riboflavin-responsive multiple acyl-CoA dehydrogenase deficiency. Brain. 2007; 130:2045–2054. [PubMed: 17584774]

Rinaldo, P.; Hahn, SH.; Matern, D. Inborn errors of amino acid, organic acid, and fatty acid metabolism. In: Burris, CA.; Ashford, ER.; Tietz, NW., editors. Tietz textbook of clinical chemistry and molecular diagnosis. 4th edn. WB Saunders; Philadelphia, PA: 2005. p. 2207-2247.

Santer R, Claass A, Krawinkel M, Schaub J, Ruitenbeek W. Decreased activity of respiratory-chain enzymes in glutaric aciduria type II. J Inherit Metab Dis. 1995; 18:75–6. [PubMed: 7623447]

Schiff M, Froissart R, Olsen RKJ, Acquaviva C, Vianey-Saban C. Electron transfer flavoprotein deficiency:Functional and molecular aspects. Mol Genet Metab. 2006; 88:153–158. [PubMed: 16510302]

Schmidt-Sommerfeld E, Bobrowski PJ, Penn D, Rhead WJ, Wanders RJ, Bennett MJ. Analysis of carnitine esters by radio-high performance liquid chromatography in cultured skin fibroblasts from

patients with mitochondrial fatty acid oxidation disorders. Pediatr Res. 1998; 44:210–4. [PubMed: 9702916]

Toogood HS, Leys D, Scrutton NS. Dynamics driving function: new insights from electron transferring flavoproteins and partner complexes. FEBS J. 2007; 274:5481–504. [PubMed: 17941859]

Treem WR, Sokol RJ. Disorders of the mitochondria. Semin Liver Dis. 1998; 18:237–53. [PubMed: 9773424]

Usselman RJ, Fielding AJ, Frerman FE, Watmough NJ, Eaton GR, Eaton SS. Impact of mutations on the midpoint potential of the [4Fe-4 S]+1,+2 cluster and on catalytic activity in electron transfer flavoprotein-ubiquinone oxidoreductase (ETF-QO). Biochemistry. 2008; 47:92–100. [PubMed: 18069858]

Zhang J, Frerman FE, Kim JJP. Structure of electron transfer flavoprotein-ubiquinone oxidoreductase and electron transfer to the mitochondrial ubiquinone pool. PNAS. 2006; 103:16212–16217. [PubMed: 17050691]

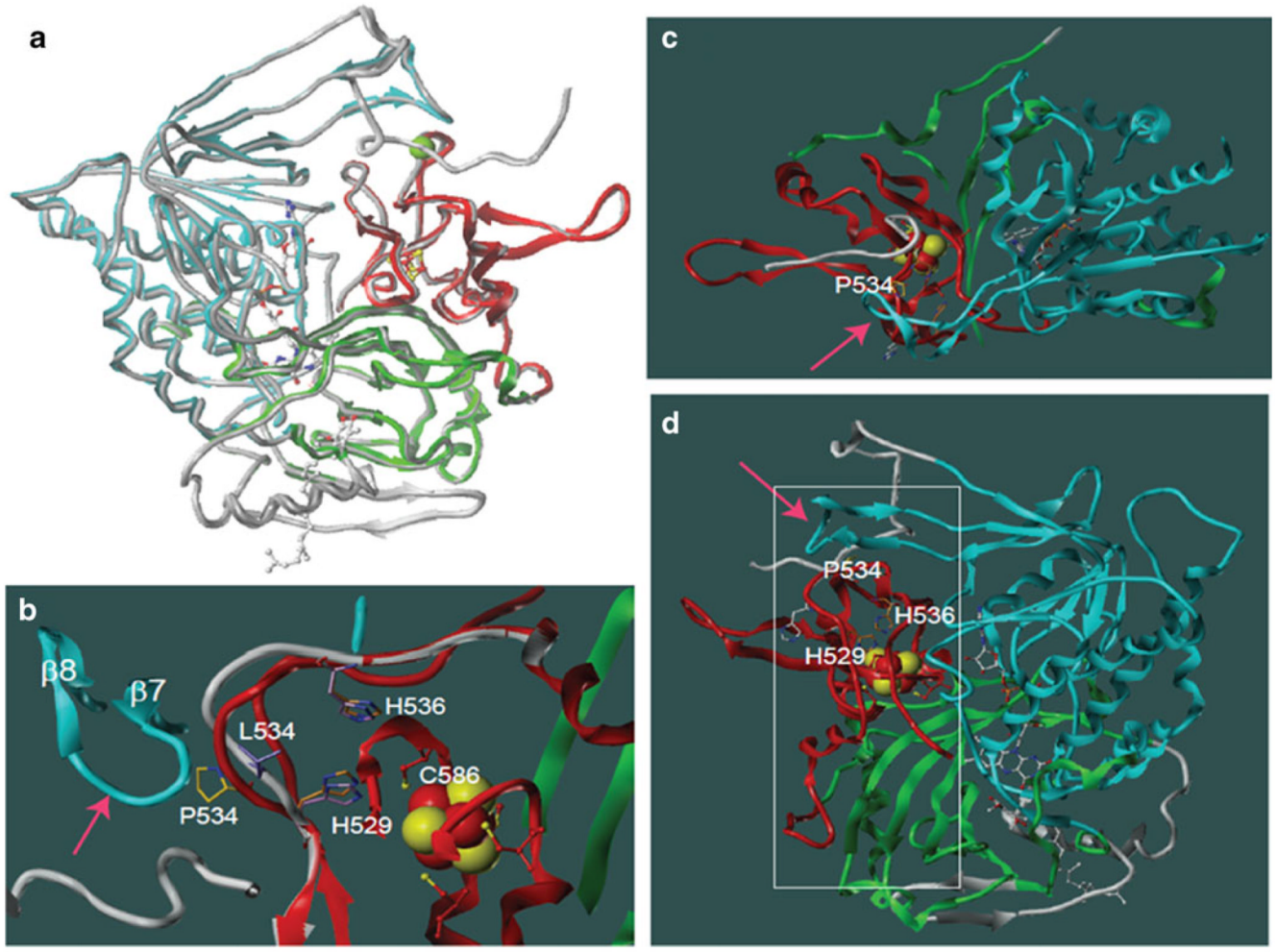

Fig. 1.

Comparative models of wild type human and mutant ETFDH P534L structures. **a**. Overlay of the crystal structure of porcine ETFDH (PDB data bank: 2GMH) and the wild type human ETFDH model. The porcine structure is highlighted in colors (red, blue and green) and the backbone of human wild type ETFDH model is shown as gray tubes. The three redox center: [4Fe-4 S]$^{2+,1+}$ cluster, FAD, and ubiquinone are shown in ball and stick representation, colored by atom color (carbon=white, oxygen=red, nitrogen=blue, sulfur= yellow, phosphorous=orange). Pro 534 is marked by a green ball on the C-alpha. Note the backbone of the human ETFDH model is nearly identical with that of the porcine structure. **b**. Close up view of the structure in which the mutation P534L resides. Side chains are displayed as stick presentation. The wild type structure is highlighted in color and the backbone of mutant model shown in gray for loop 529-536. L534 in the mutant model is highlighted in purple. The carbons in P534 of the wild type structure are shown in yellow. The carbons H536 and H529 of the mutant model are colored in magenta and the wild type in gold. Cys 586 is depicted in ball and stick model, and those carbons are red, sulfurs are yellow. Note that Cys 586 directly interacts with H529. If the conformation of the backbone of β 7 and 8 loops (shown by the arrow) in the mutant stays unchanged, the shift of loop 529-536 in the mutant could induce up to 1 angstrom rotation of the side chain of H529 due to the P534L mutation. **c**. The crystal structure of porcine ETFDH displayed as in panel A, but rotated 90 degrees. The arrow points to the potential binding site at the bottom, showing

the large surface area depicted in panel D that is flat. Note the loop containing Pro 534 is relatively exposed. **d**. Another view of the wild type structure highlights the external surface of the molecule. The potential ETF binding site is to the left of the molecule and angles toward the front as shown by a white square. Note the position of P534 and its close relation to the surface conformation through β 7 and 8 (shown by the pink arrow) and its proximity to the iron-sulfur cluster through His 529 and His 536 that reside on the loop in which P534 also resides

Table 1

Activities of oxidative phosphorylation complexes in homogenates of liver and skeletal muscle (all activities μmol/min/g wet weight tissue)

Enzyme	Tissue	Control	Patient (% control mean)
Complex I	SM	29.9±12.9 (11.5-60.1)	16.7 (56)
	L	64.4±20.3 (41.2-78.4)	78.4 (122)
Complex II	SM	0.8±0.4 (0.1-2.0)	0.1(6)
	L	4.1 ±1.5 (2.9-5.7)	0 (0)
Complex III	SM	15.2±6.8 (6.8-35.2)	1.7(11)
	L	63.2±64.8 (17.4-109)	2.6 (4)
Complex IV	SM	148.9±67.2 (57.3-373)	0 (0)
	L	49.3±62.4 (0.1-130)	38.6 (78)
CS	SM	18.6±4.7 (9.4-30)	6.2 (33)
	L	7.9±2.2 (5.3-10.6)	6.1(78)

Complex I=NADH-ferricyanide reductase;

Complex II=succinate dehydrogenase;

Complex III=decylubiquinol-cytochrome c reductase;

Complex IV=cytochrome oxidase; CS=citrate synthase;

SM=skeletal muscle;

L=Liver;

parenthetical values in the control column indicate range (mean±SD; n=49 for skeletal muscle and n=4 for liver).

Table 2

Activities of acyl-CoA dehydrogenases and related fatty acid oxidation enzymes in homogenates of liver and skeletal muscle (all activities μmol/min/g wet weight tissue)

Enzyme	Tissue	Control	Patient (% control mean)
SCAD (C4)	SM	0.94±0.36 (0.44-1.95)	0.44 (46)
	L	4.6±2.95 (2.48-8.92)	2.16 (47)
MCAD (C8)	SM	0.88±0.22 (0.61-1.31)	0.69 (78)
	L	2.15±0.38 (1.87-2.7)	2.55 (119)
LCAD (C16)	SM	1.22±0.44 (0.67-2.29)	0.58 (47)
	L	2.52±0.94 (1.46-3.64)	1.26 (50)
3-Hydroxy-ACD (C4)	SM	18.51 ±8.25 (6.0-37.45)	15.62 (84)
	L	17.31 ±5.51 (9.75-24.8)	20.54 (119)
Ketothiolase (C4)	SM	9.61 ±3.48 (4.6-16.8)	0.5 (5)
	L	24.95±2.46 (20.95-27.35)	10.18 (41)
CS	SM	15.56±3.87 (11.35-24.2)	6.23 (40)
	L	7.03±2.53 (5.05-11.85)	6.12 (87)

SCAD=short chain acyl-CoA dehydrogenase;

MCAD=medium chain acyl-CoA dehydrogenase;

LCAD=long chain acyl-CoA dehydrogenase;

3-hydroxy-ACD=3-hydroxyacyl-CoA dehydrogenase;

ketothiolase=short chain beta-ketothiolase;

SM=skeletal muscle;

L=liver; values for control represent mean±SD with range in parenthesis (n=25 for skeletal muscle, n=8 for liver).